

# The chain length of anisotropic paramagnetic particles in a rotating field

Jānis Užulis and Jānis Čīmurs\*

*Laboratory of Magnetic Soft Materials*

*Faculty of Physics, Mathematics and Optometry*

*University of Latvia*

*Jelgavas iela 3-530,*

*Riga, Latvia, LV-1004*

(Dated: June 24, 2022)

## Abstract

In this article maximal length of a chain of paramagnetic particles with magnetic anisotropy in a rotating magnetic field is studied. The theory of paramagnetic particle chains usually assumes that the particles are magnetically isotropic and do not rotate in a rotating field. In experiments it is seen that spherical paramagnetic particles rotate, what can be explained by small magnetic anisotropy. In this article, the maximal chain length is calculated for paramagnetic particles with magnetic anisotropy in a rotating magnetic field. Results show that the maximal chain length as a function of field frequency has the same trend for isotropic magnetic particles and particles with magnetic anisotropy if the field frequency is much higher or much lower than the critical frequency of an individual particle. A large number of initially randomly distributed particles will form a large number of chains. The chains will collide and exchange with particles till obtain a typical chain length of the ensemble. The typical chain length of the ensemble is shorter than the maximal chain length of individual chain for the same field frequency. The distribution of chain lengths in an ensemble of chains is narrower for particles with higher magnetic anisotropy. Due to the narrower distribution of chain lengths, particles with magnetic anisotropy can suit better for mass-production. This article will show how magnetic anisotropy parameters of paramagnetic particles influence chain length of chains which form in a rotating magnetic field.

## I. INTRODUCTION

It is shown that paramagnetic particles in a rotating magnetic field becomes attractive [1, 2]. If the field frequency is small particles form chains [1, 3] where chain length depends on the field frequency [4–7] and fluid and particle parameters.

Magnetic particles chains can be used for cargo transport [2, 8]. The advantage of the magnetic particles in cargo transport is that the motion can be fully controlled from the outside using a pattern of an external magnetic field. Functionalized magnetic particles can be linked together creating magnetic filament [9, 10] which can be used as magnetic swimmer [11]. For these applications the possibility of creating large amount of chains with well defined length is advantageous.

---

\* janis.cimurs@lu.lv; mmml.lu.lv

Magnetic fluid which consists of superparamagnetic particles suspended in a liquid also exhibits similar formation of chains in a rotating magnetic field [12, 13]. Despite the fact that in a phase separated magnetic fluid surface tension and thermal motion of the particles play important role, behaviour of magnetic fluid in rotating field is similar to behaviour of an ensemble of magnetic particles. In slow rotating magnetic field magnetic fluid forms elongated drops with narrow distribution of lengths [12].

The theory of spherical paramagnetic particles in a rotating magnetic field usually do not take into account magnetic anisotropy of particles, therefore particles are assumed non-rotating. In reality it can be seen that paramagnetic particles rotate in a rotating field [2, 14]. In these articles rotation of spherical paramagnetic particles is explained by finite relaxation time of magnetic moment. The rotation of the paramagnetic particles can be explained also by magnetic anisotropy of the susceptibility of the particles.

In this article chain formation of paramagnetic particles with anisotropy in a rotating magnetic field is investigated. Critical chain length is compared to theory for chains of isotropic paramagnetic particles to see if measurable difference can be observed. Also hypothesis that particles with magnetic anisotropy have more narrow chain length distribution in initially randomly distributed ensemble of particles is tested. The results and conclusions show advantages for using paramagnetic particles with anisotropy to form paramagnetic chains.

## II. MODEL

In this article we will use paramagnetic particles with spherical form and with uniaxial magnetic anisotropy. The magnetic anisotropy could be due to the crystallographic structure [15] or particles are not ideally spherical or particle could be magnetic rod in a spherical shell [16] or magnetic Janus particles, where some regions has different magnetic susceptibility [17]. When the particles are subjected to a weak magnetic field  $\vec{H}$  the magnetic dipole moment  $m_i$  is induced in each particle. The dipole moment of  $i$ -th particle can be calculated using a linear particle magnetisation and field relation:

$$\vec{m}_i = V_m \left( \chi_{\perp} \vec{H}_i + \Delta\chi (\vec{n}_i \cdot \vec{H}_i) \vec{n}_i \right) , \quad (1)$$

where  $V_m$  is the magnetic volume of the particle,  $\vec{H}_i$  is the magnetic field at the point of the particle,  $\vec{n}_i$  is the unit vector in the direction of the anisotropy axis of the particle,  $\Delta\chi = \chi_{\parallel} - \chi_{\perp}$  is difference of the magnetic susceptibilities, where  $\chi_{\parallel}$  and  $\chi_{\perp}$  are magnetic susceptibility of the particle in the direction of anisotropy axis and perpendicular to it respectively. For ellipsoidal paramagnetic particles susceptibilities  $\chi_{\perp}$  and  $\chi_{\parallel}$  are related to material susceptibility as shown by Stoner [18]. For example spherical particle with infinite magnetic susceptibility has  $\chi_{\parallel} = \chi_{\perp} = 3$ . Parameter  $\frac{\chi_{\parallel}}{\chi_{\perp}}$  is used to characterize the anisotropy of the particle in this article. The direction of magnetization  $\vec{m}$  is illustrated in figure 1 for different external field  $\vec{H}$  and anisotropy axis  $\vec{n}$  configurations.

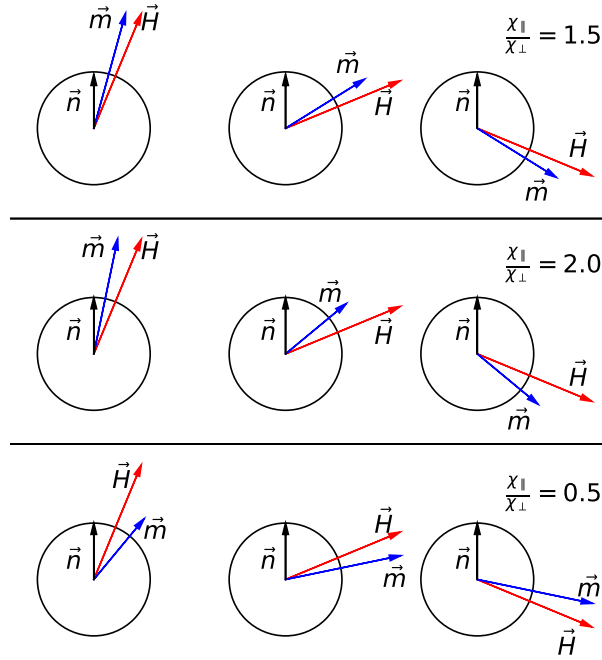


FIG. 1. Magnetic moment  $\vec{m}$  direction depending on the magnetic field  $\vec{H}$  direction. The magnetization  $|\vec{m}|$  is normalized to the field strength  $|\vec{H}|$  for each anisotropy case. In upper two examples  $\vec{n}$  is an easy magnetization axis ( $\frac{\chi_{\parallel}}{\chi_{\perp}} = 2$ ,  $\frac{\chi_{\parallel}}{\chi_{\perp}} = 1.5$ ) and in the lower one example  $\vec{n}$  is a hard magnetization axis ( $\frac{\chi_{\parallel}}{\chi_{\perp}} = 0.5$ ). The direction of the magnetization  $\vec{m}$  and the external field  $\vec{H}$  direction coincide when the direction of  $\vec{H}$  is along anisotropy axis  $\vec{n}$  or perpendicular to it.

The figure 1 shows that magnetization  $\vec{m}$  is closer to anisotropy axis if  $\chi_{\parallel} > \chi_{\perp}$  and anisotropy axis is an easy axis. If  $\chi_{\perp} > \chi_{\parallel}$  the anisotropy axis is a hard axis and magnetization of the particle is closer to the equator of the particle.

In the model these particles are dispersed in liquid with viscosity  $\eta$ . Each particle rotates due to torque  $\vec{\tau}_i = \mu_0 \vec{m}_i \times \vec{H}_i$  which is compensated by viscous drag. The rotation of the particle can be calculated as [19]:

$$\frac{d\vec{n}}{dt} = \frac{\mu_0 V_m \Delta \chi}{\xi_r} \left( \vec{n} \cdot \vec{H}_i \right) \left[ \vec{H}_i - \left( \vec{n} \cdot \vec{H}_i \right) \vec{n} \right], \quad (2)$$

where  $\vec{n}$  is magnetic anisotropy axis, which is fixed to the particle,  $\mu_0$  is magnetic constant (vacuum permeability),  $\xi_r = 8\pi\eta R^3$  is rotational drag coefficient, where  $R$  is hydrodynamic radius of the particle and  $\eta$  is viscosity of the liquid. It is assumed that viscosity dominates over inertia and Reynolds number is below unity and inertial term can be neglected.

The magnetic field at the point of the particle  $\vec{H}_i$  is a sum of the external field  $\vec{H}$  and the field produced by all other particles.  $j$ -th particle at the point of  $i$ -th particle produces field:

$$\vec{H}_{ij}(\vec{r}_{ij}) = \frac{1}{4\pi} \left( \frac{3\vec{r}_{ij}(\vec{m}_j \cdot \vec{r}_{ij})}{r_{ij}^5} - \frac{\vec{m}_j}{r_{ij}^3} \right). \quad (3)$$

where  $\vec{r}_{ij} = \vec{r}_i - \vec{r}_j$  is distance vector from the point of  $j$ -th particle to the point of  $i$ -th particle. The magnetic field at the point of the  $i$ -th particle is  $\vec{H}_i = \vec{H} + \sum_j \vec{H}_{ij}$

Since the field produced by particles is not homogeneous, particles also move. The force exerted by  $j$ -th particle on the  $i$ -th particle can be calculated as

$$\begin{aligned} \vec{F}_{ij,M} = \frac{3\mu_0}{4\pi r_{ij}^5} & \left[ (\vec{m}_i \cdot \vec{r}_{ij}) \vec{m}_j + (\vec{m}_j \cdot \vec{r}_{ij}) \vec{m}_i \right. \\ & \left. + (\vec{m}_i \cdot \vec{m}_j) \vec{r}_{ij} - \frac{5(\vec{m}_i \cdot \vec{r}_{ij})(\vec{m}_j \cdot \vec{r}_{ij})}{r_{ij}^2} \vec{r}_{ij} \right]. \end{aligned} \quad (4)$$

The non-overlap of the particles is fulfilled using repulsive part of Lenard-Jones potential. Repulsive force is:

$$\vec{F}_{ij,R} = \begin{cases} -G \left( \frac{1}{r_{ij}^{13}} - \frac{r_{ij}-2R}{r_{max}-2R} \frac{1}{r_{max}^{13}} \right) \frac{\vec{r}_{ij}}{r_{ij}} & \text{if } r_{ij} \leq r_{max} \\ 0 & \text{if } r_{ij} > r_{max} \end{cases}. \quad (5)$$

The repulsive force is proportional to the particle distance in power of  $-13$  as obtained from Lenard-Jones potential repulsion part. Constant  $G$  is chosen so that the maximal attractive magnetic force  $\vec{F}_{ij,M}$  between two particles at the distance of  $|r_{ij}| = 2R$  between particles centers is compensated by repulsive force  $\vec{F}_{ij,R}$  and  $\vec{F}_{ij,M,max} + \vec{F}_{ij,R} = 0$ . The maximal attractive magnetic force is obtained in situation where  $\vec{n}_i \parallel \vec{H}_i$  and  $\chi_{\parallel} > \chi_{\perp}$  and  $\vec{r}_{ij} \parallel \vec{m}_i \parallel \vec{m}_j$ . The maximal magnetic force is  $\vec{F}_{ij,M,max} = \frac{3V_m^2 \chi_{\parallel}^2 H_i^2 \mu_0}{32\pi R^4}$  and consequently  $G = F_{ij,M,max}(2R)^{13}$ .

The parameter  $r_{max}$  is a bit larger than  $2R$  and determine the softness of the particle. The equation part  $\frac{r_{ij}-2R}{r_{max}-2R} \frac{1}{r_{max}^{13}}$  makes the repulsive force 0 at the particle distance  $r_{ij} = r_{max}$  and makes the repulsion function without steps, to avoid numerical instabilities.

The sum of all forces, the magnetic force (4) and the repulsive force (5), will cause the particle to move. In the non-inertial limit the driving force is compensated by drag force for spherical particle  $\vec{F}_D = -6\pi\eta R\vec{v}$ , where  $\vec{v}$  is velocity of the particle. Velocity of the  $i$ -th particle is calculated as:

$$\vec{v}_i = \frac{1}{6\pi\eta R} \sum_j \vec{F}_{ij}, \quad (6)$$

where  $\vec{F}_{ij} = \vec{F}_{ij,M} + \vec{F}_{ij,R}$  is a sum of all the forces.

Magnetic particles are subjected by an external rotating magnetic field:  $\vec{H} = H(\cos(\omega_H t), \sin(\omega_H t), 0)$ , where  $\omega_H$  is a field rotation frequency.

### III. THEORY

The theory by Melle et al [4] shows that isotropic particles in a slow rotating magnetic field form chains with length proportional to  $\frac{1}{\sqrt{\omega_H}}$ . In this article we will show that if particle has an anisotropy of magnetic susceptibility, then the chain length in rotating magnetic field deviates from the trend  $\frac{1}{\sqrt{\omega_H}}$  if the frequency is close to critical.

Isolated paramagnetic particle rotates synchronously with the field if  $\omega_H < \omega_{C,1}$  [20], where

$$\omega_{C,1} = \frac{\mu_0 V_m \Delta \chi H^2}{2\xi_r} = \frac{\mu_0 V_m \Delta \chi H^2}{16\pi\eta R^3}$$

and  $H$  is the field strength of the external magnetic field. If particles magnetic anisotropy axis is hard axis ( $\chi_{\parallel} < \chi_{\perp}$ ) then anisotropy axis lay perpendicularly to the plane of the rotation of the magnetic field and the directions of  $\vec{m}$  and  $\vec{H}$  coincide. The rotation of the particle is no longer happening and the chain formation is the same as for isotropic particles where chain length, as shown by Miele et al [4], is proportional to  $\frac{1}{\sqrt{\omega_H}}$ .

#### A. Slow field

For particles with magnetic anisotropy easy axis ( $\chi_{\parallel} > \chi_{\perp}$ ), anisotropy axis is in the plane of the rotating field and magnetic moment of the particle depend on the angle between

the external field  $\vec{H}$  and a anisotropy axis of a particle  $\vec{n}$ . In a slow rotating magnetic field  $\omega_H < \omega_{C,1}$  particle follows the field and a magnetic moment of a particle is constant:

$$|\vec{m}| = V_m \sqrt{\chi_{\perp}^2 \vec{H}^2 + 2\chi_{\perp} \Delta\chi (\vec{n} \cdot \vec{H})^2 + \Delta\chi^2 (\vec{n} \cdot \vec{H})^2},$$

where [19]

$$(\vec{n} \cdot \vec{H})^2 = \frac{H^2}{2} \left( 1 + \sqrt{1 - \left( \frac{\omega_H}{\omega_{C,1}} \right)^2} \right).$$

From the theory of Miele et al [4] chain will break if the angle between the chain and the external magnetic field exceeds critical value  $\frac{\pi}{4}$ . In other words, chain will break if hydrodynamic drag  $6\pi\eta R^2 \omega_H N^2$  will overcome magnetic force  $\frac{3\mu_0}{4\pi(2R)^4} |\vec{m}|^2$ . Putting all together, it gives formula for chain length in a slow rotating field with field frequency  $\omega_H$ :

$$N = \sqrt{\frac{V_m \omega_{C,1}}{\Delta\chi 16\pi R^3 \omega_H}} \sqrt{\chi_{\perp}^2 + \chi_{\parallel}^2 + (\chi_{\parallel}^2 - \chi_{\perp}^2) \sqrt{1 - \frac{\omega_H^2}{\omega_{C,1}^2}}} \quad (7)$$

It can be shown that chain length  $N$  deviates from trend  $N \propto \frac{1}{\sqrt{\omega_H}}$  only for values of  $\frac{\omega_H}{\omega_{C,1}}$  close to unity. If rotation frequency is small ( $\omega_H \ll \omega_{C,1}$ ) Equation (7) becomes

$$N = \sqrt{\frac{V_m \chi_{\parallel}^2}{8\pi \Delta\chi R^3}} \sqrt{\frac{\omega_{C,1}}{\omega_H}} = \sqrt{\frac{\mu_0 V_m^2 H^2 \chi_{\parallel}^2}{16\pi \xi_r R^3}} \sqrt{\frac{1}{\omega_H}},$$

which is proportionality  $N \propto \frac{1}{\sqrt{\omega_H}}$ . For particles, which are almost spherical, the critical rotation frequency  $\omega_{C,1}$  can become extremely small and frequencies  $\omega_H$  corresponding to  $N > 1$  are much higher than the critical frequency  $\omega_{C,1}$  and formula (7) is not suitable.

## B. Fast field

Particles, which are almost isotropic, has low critical field frequency  $\omega_{C,1}$  and do not follow the field. This regime is called asynchronous rotation because the angle between external field  $\vec{H}$  and particle direction  $\vec{n}$  changes. Numerical simulations show that, if the field frequency is large enough, particles synchronise with each other.

The force between two neighbouring synchronised particles would be:

$$\vec{F}_{ij} = \frac{3\mu_0}{4\pi(2R)^4} [2(\vec{m} \cdot \hat{r})\vec{m} + \vec{m}^2 \hat{r} - 5(\vec{m} \cdot \hat{r})^2 \hat{r}] , \quad (8)$$

where attractive radial force is

$$F_r = \frac{3\mu_0}{4\pi(2R)^4} [\vec{m}^2 - 3(\vec{m} \cdot \hat{r})^2]$$

and the force which makes particles to rotate along common center is

$$\vec{F}_\theta = \frac{3\mu_0}{2\pi(2R)^4} (\vec{m} \cdot \hat{r})(\vec{m} \cdot \hat{\theta}) ,$$

where  $\hat{r}$  is a unit vector in the direction to the other particle and  $\hat{\theta}$  is a unit vector perpendicular to  $\hat{r}$  and in the direction of the rotation. Using Eq. (1) and introducing angle  $\theta$  between  $\vec{H}$  and  $\vec{r}$  and angle  $\varphi$  between  $\vec{n}$  and  $\hat{r}$  gives relations for magnetic moment  $\vec{m}$ :

$$\begin{aligned} \hat{r} \cdot \vec{m} &= V_m H \left( \chi_\perp \cos \theta + \Delta \chi \cos \varphi \cos(\theta - \varphi) \right) \\ \vec{m}^2 &= V_m^2 H^2 \left( \chi_\perp^2 + (\chi_\parallel^2 - \chi_\perp^2) \cos^2(\theta - \varphi) \right) \\ \vec{m} \cdot \hat{\theta} &= V_m H \left( -\chi_\perp \sin \theta + \Delta \chi \sin \varphi \cos(\theta - \varphi) \right) \end{aligned}$$

It will be assumed that in high frequency  $\theta$  changes slowly and  $\varphi$  increases linearly with time. This gives possibility to average trigonometric functions over linearly increasing  $\varphi$ . The average inter-particle force will read

$$\begin{aligned} \langle F_r \rangle &= -\frac{3\mu_0 V_m^2 H^2}{32\pi(2R)^4} (2(\chi_\perp^2 + \chi_\parallel^2) + 3(\chi_\perp + \chi_\parallel)^2 \cos(2\vartheta)) \\ \langle F_\theta \rangle &= -\frac{3\mu_0 V_m^2 H^2}{16\pi(2R)^4} (\chi_\perp + \chi_\parallel)^2 \sin(2\vartheta) \end{aligned}$$

For reasonable  $\frac{\chi_\parallel}{\chi_\perp}$ , the average force is close to isotropic situation, where  $\chi_\parallel = \chi_\perp$ .

The conclusion in high frequency range is similar to the conclusion for isotropic particles [4]. In anisotropic situation the angle  $\theta$ , at which  $\langle F_r \rangle$  becomes repulsive, is larger than the magic angle, for any  $\frac{\chi_\parallel}{\chi_\perp}$  value. Therefore, breakage of the chain will happen when friction force will overcome maximal  $\langle F_\theta \rangle$ . As a result, maximal chain length in high frequency range is:

$$N = \sqrt{\frac{\mu_0 V_m^2 H^2 (\chi_\parallel + \chi_\perp)^2}{64\pi R^3 \xi_r}} \sqrt{\frac{1}{\omega_H}} \quad (9)$$

As can be seen, in high frequencies, chain length also is proportional to  $\frac{1}{\sqrt{\omega_H}}$ .

When the field frequency gets close to critical frequency, the given equation of chain length Eq. 9 will not work. To calculate more precise relation the back and forth rotation of each



particle should be considered in the derivation, which gives field frequency dependent mean values for trigonometric functions of  $\varphi$ . For example, mean value  $\langle \sin(2\varphi) \rangle = \frac{\omega_H - \sqrt{\omega_H^2 - \omega_{C,1}^2}}{\omega_{C,1}}$  [20]. In addition, in asynchronous rotation of the particles, the assumption does not hold that the angle  $\theta$  between the chain and the field does not change does not hold. The fact that the angle  $\theta$  changes does not allow to obtain maximal chain length in closed form in medium frequencies in asynchronous regime.

### C. Long chain correction

The results obtained so far was based on the assumption that farther particles does not influence magnetic field of middle particles. This is not true even for two particles. For longer chains the influence of all particles should be considered. Usually infinitely long chain is considered. In infinitely long straight chain the force and the torque on each particle can be calculated and they involves two angles ( $\varphi$  and  $\theta$ ) in different trigonometric combinations. This does not allow to obtain solution in closed form even for low field frequencies. In simulations it can be seen that chain is not straight but S-shape. As a result, further analysis of chain lengths is based on simulations results.

## IV. RESULTS AND DISCUSSIONS

The model described in section II was implemented in a C++ computer program, to do numerical simulations. Translation motion Eq.(6) and rotation motion Eq.(2) for each particle is being calculated by solving first order ordinary differential equation system of  $6N$  equations where  $N$  is number of particles. GNU Scientific Library [21], Runge-Kutta 4th order method with adaptive time step were used to solve the differential equation system.

### A. Soft VS hard particles

By choosing parameter  $r_{max}$  value in Eq.(5), steepness of the repulsion force function can be regulated. The smaller  $r_{max}$  value we choose the steeper is grow of the repulsive force as can be seen in Fig. 2.

If there is a chain of two particles (a dimer) and the third particle comes closer to the

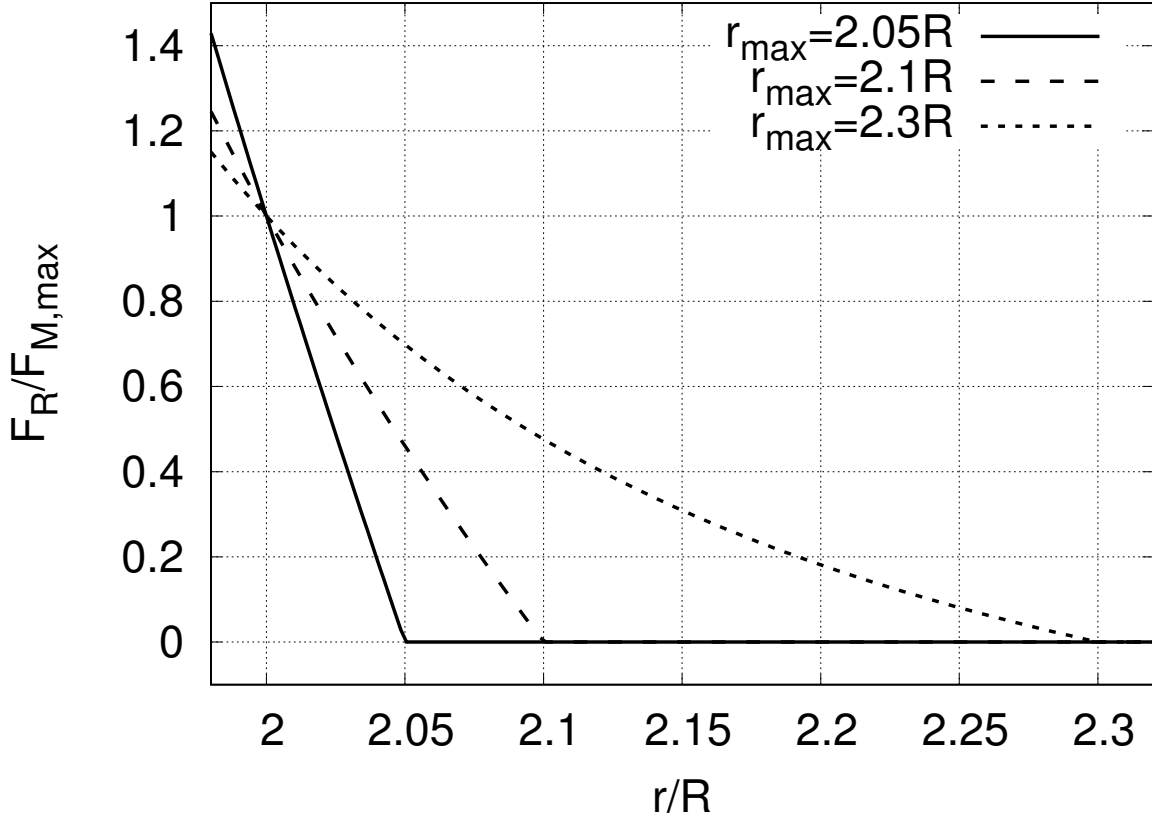


FIG. 2. Repulsive force Eq. (5)  $F_R$  depending on particle distance  $r$ , with different parameter  $r_{max}$ , normalized to maximal magnetic force of two particles at distance  $2R$ . Steepness of the repulsive force function  $F_R$  (the softness of the particle) can be regulated by choosing parameter  $r_{max}$ .

dimer, like illustrated in Fig.3, the magnetic force acting on the third particle is repulsive if its position  $x > 2R$ . If the third particle position  $x < 2R$  then the magnetic force on the third particle is attractive to the dimer and they form trimer. Distance between the center of third particle and the line of centers of dimer particles, where the force changes direction, is  $\sqrt{5}R$ . If the value of  $r_{max}$  is larger than  $\sqrt{5}R$  then in ensemble of particles the probability for particles to form a trimer is small and these three particle will form a chain structure. The increase of  $r_{max}$  not only increase the distance of repulsive force but also makes particles more soft. The particles close to each other amplify the field and repulsive force at the distance  $2R$  does not compensate attractive magnetic force completely and the force equilibrium distance is at a distance a bit less than  $2R$ , that makes the force acting on

third particle flip direction at a distance a bit less than  $\sqrt{5}R$ . If larger  $r_{max}$  value is used the particles are softer than with small  $r_{max}$  value.

In an article [22] order of the chain in external field is being regulated by salt concentration in the liquid, the higher the salt concentration the less disordered the chain gets. In our model similar structural effects are observed by changing  $r_{max}$  value. Higher  $r_{max}$  value corresponds a to higher salt concentration

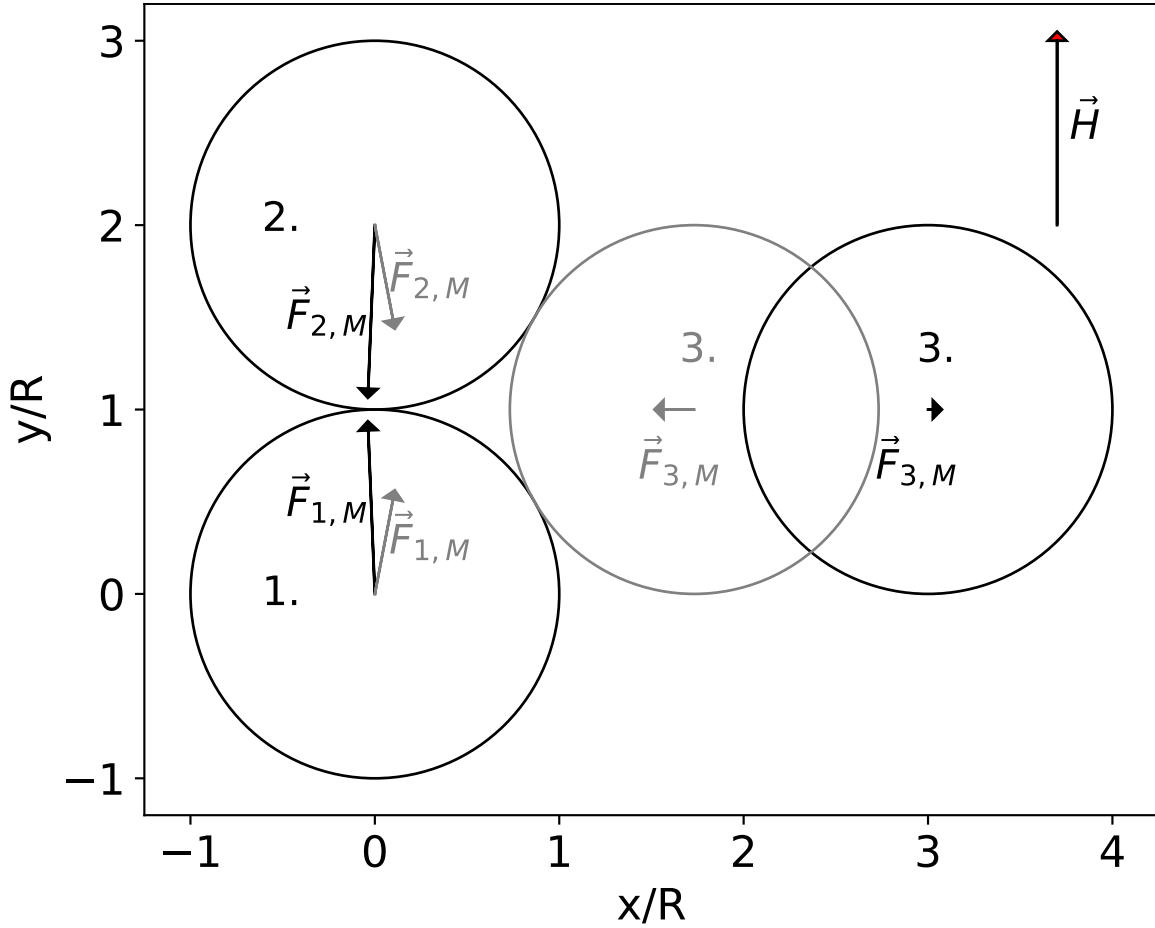


FIG. 3. Two particle chain and a situation where the third particle is at a distance where the force is repulsive (particle and forces in black) and a situation where the third particle is at a distance where the force is attractive to the chain (particle and forces in gray). Sizes of the force vectors are drawn in a scale where  $F_{i,M,max} = 1$ .

## B. Critical length of a single chain

At the beginning,  $N$  particles are placed in a straight chain along the direction of a stationary field. At this phase particles obtain equilibrium distance between each other. Then the field starts to rotate with a certain frequency  $\omega_H$ . If the frequency is higher than the critical frequency  $\omega_{C,N}$ , the chain breaks after some periods, but, if the frequency is below critical - the chain does not break. There is a very well observable boundary between the frequency where the chain breaks in a few periods and the frequency where the chain does not break in even a couple of hundred periods.

Angle between the line of the end particles of the chain and the external field (Fig.4) is being monitored to detect when the chain breaks. If the angle gets larger than  $\frac{\pi}{2}$  then the chain is definitely broken. By monitoring this angle even breaking of a two particle chain can be detected.

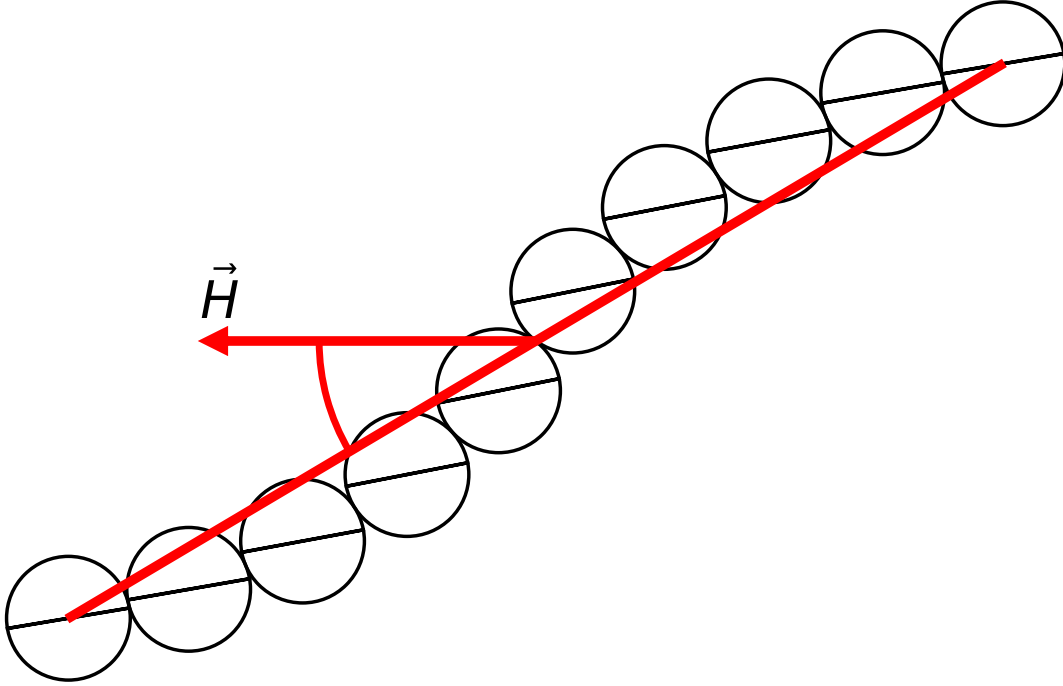


FIG. 4. S-shaped chain at critical field rotation frequency  $\omega_{C,10}$ . Angle between the line of the end particles of the chain and the external field  $\vec{H}$  is being monitored to detect breaking of the chain. The field rotates clockwise. Easy magnetisation axis is shown as a black line in a particle.

If the field rotation frequency  $\omega_H$  is slightly smaller than the critical rotation frequency

$\omega_{C,N}$  for given chain 4 structurally different rotation regimes can be observed. If  $\omega_H < \omega_{C,1}$ , then each particle rotates synchronously with the field (mode 1. Fig.5). If  $\omega_H$  is above  $\omega_{C,1}$ , then two scenarios can be observed. In the first scenario, the end particles of the chain start to lag behind the field and their rotation becomes asynchronous with the field but the middle particles rotate synchronously with the field (mode 2.a Fig. 5). In the second scenario, the middle particle of the chain start to lag the field (mode 2.b Fig. 5). If the frequency is increased further, then more than two particles rotate asynchronously with the field, and the rotation of middle particles is faster than the rotation of the end particles (mode 3. Fig. 5). If the field frequency is increased even more, then the rotation frequency for all particles become so small that it can be assumed that the particles synchronize (mode 4. Fig. 5). Visual representation of all modes can be found in the supplementary video.

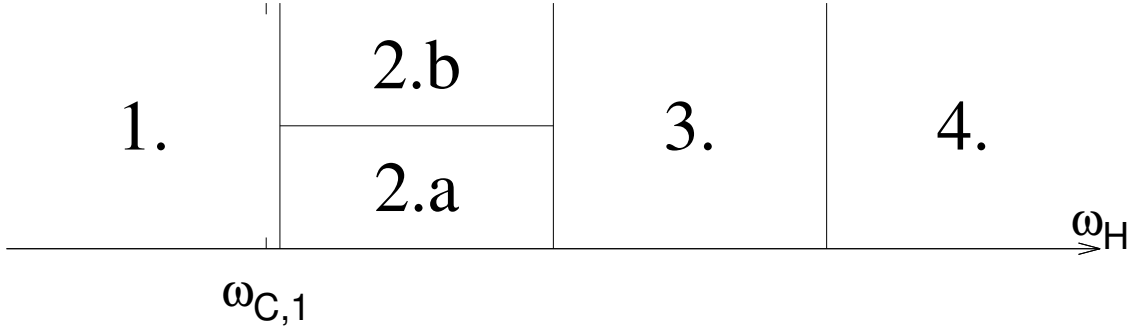


FIG. 5. Chain rotation mode classification depending on the field rotation frequency  $\omega_H$  if the field rotation frequency is close to the critical frequency  $\omega_{C,N}$ . **1.** Synchronous mode (each particle rotates synchronously with the field). **2.a** Both end particles rotate asynchronously with the field. **2.b** Middle particle of the chain rotates asynchronously with the field. **3.** More than two particles rotate asynchronously with the field and their rotation frequencies do not match. **4.** All particles rotate slower than the the field and they rotate synchronously with each other. All modes in video format can be found in supplementary materials.

Fig.6 shows critical chain length  $N$  dependence on the field frequency for particles with different magnetic anisotropy properties. For particles with  $\frac{\chi_{\parallel}}{\chi_{\perp}} = 1.5$  and  $\chi_{\parallel} = 2$  there is a transition between mode 1. and mode 2.a for a chain length of 13 and 12 particles (a 13 particles chain at its critical frequency  $\omega_{C,13} = 1.49$  rotates in mode 1 and a 12 particle chain at its critical frequency  $\omega_{C,12} = 1.6$  rotates in mode 2.a). This mode change is not

particularly pronounced in Fig. 6 if the chain is long but for a shorter chains, like in example  $\frac{\chi_{\parallel}}{\chi_{\perp}} = 1.5$  and  $\chi_{\parallel} = 0.25$ , the mode transition is visible as a step in a plot between chain length of 5 and 4 particles.

For particles  $\frac{\chi_{\parallel}}{\chi_{\perp}} = 1.25$  and  $\chi_{\parallel} = 0.5$  there is a transition from mode 1. to mode 2.b at chain length of 10 to 9, and an 8 particle chain rotates in mode 3. Transition between mode 2.a and mode 3. is visible in example  $\frac{\chi_{\parallel}}{\chi_{\perp}} = 1.5$  and  $\chi_{\parallel} = 2$  for a chain length of 10 and 9 particles. Steepness of the plot changes as the mode changes.

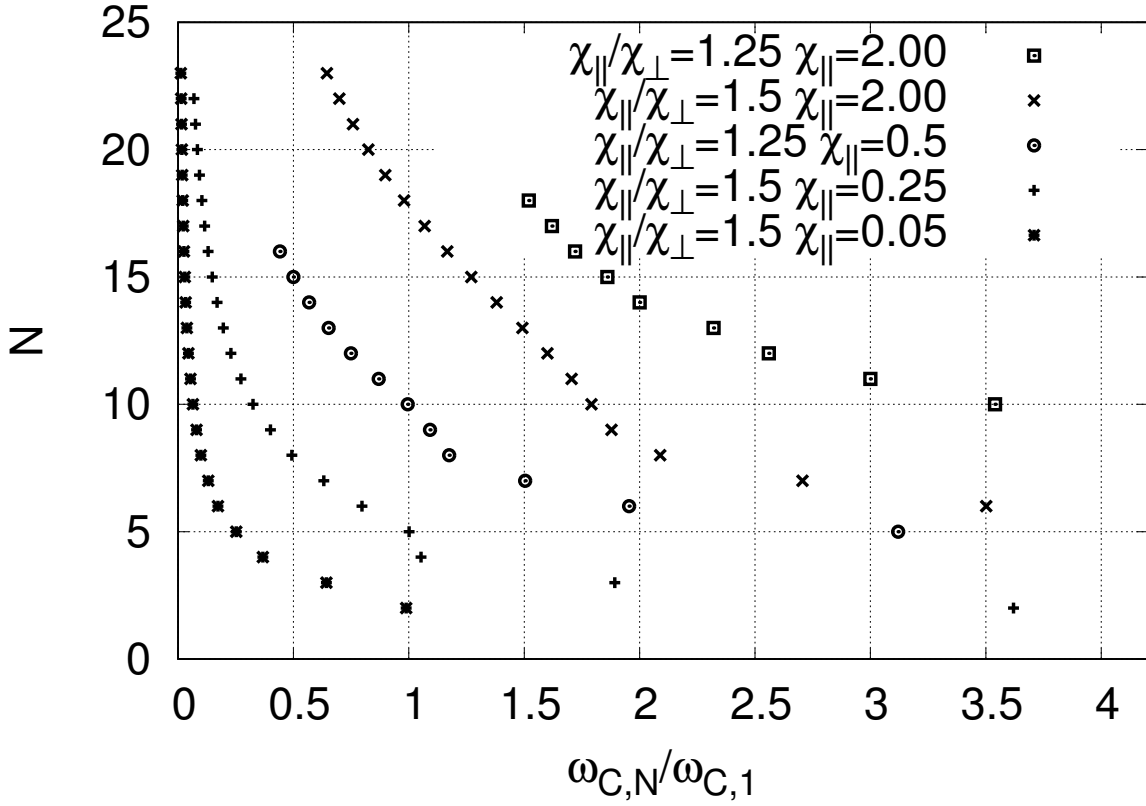


FIG. 6. Chain length  $N$  and its critical field rotation frequency  $\frac{\omega_{C,N}}{\omega_{C,1}}$  for chains with different magnetic anisotropy properties. Transitions between chain rotation modes are visible like step or change of steepness of the graph.

For particles with low  $\omega_{C,1}$ , which corresponds to almost isotropic particles, where  $\frac{\omega_{C,N}}{\omega_{C,1}} > 4$ , mode 4. are observed. Critical chain length in mode 4. can be well approximated as function proportional to  $\frac{1}{\sqrt{\omega_{C,N}}}$ . In Fig.7 linear fit is shown for critical chain length for chains where critical chain length is in mode 4. In Fig.7 for susceptibility values  $\chi_{\parallel}/\chi_{\perp} = 1.5$

and  $\chi_{\parallel} = 2$  also linear fit in region  $\omega_{C,N}/\omega_{C,1} > 1$  where critical chain is in mode 1. can be observed. The linear fits have different slopes in mode 1. and mode 4. for the same particles.

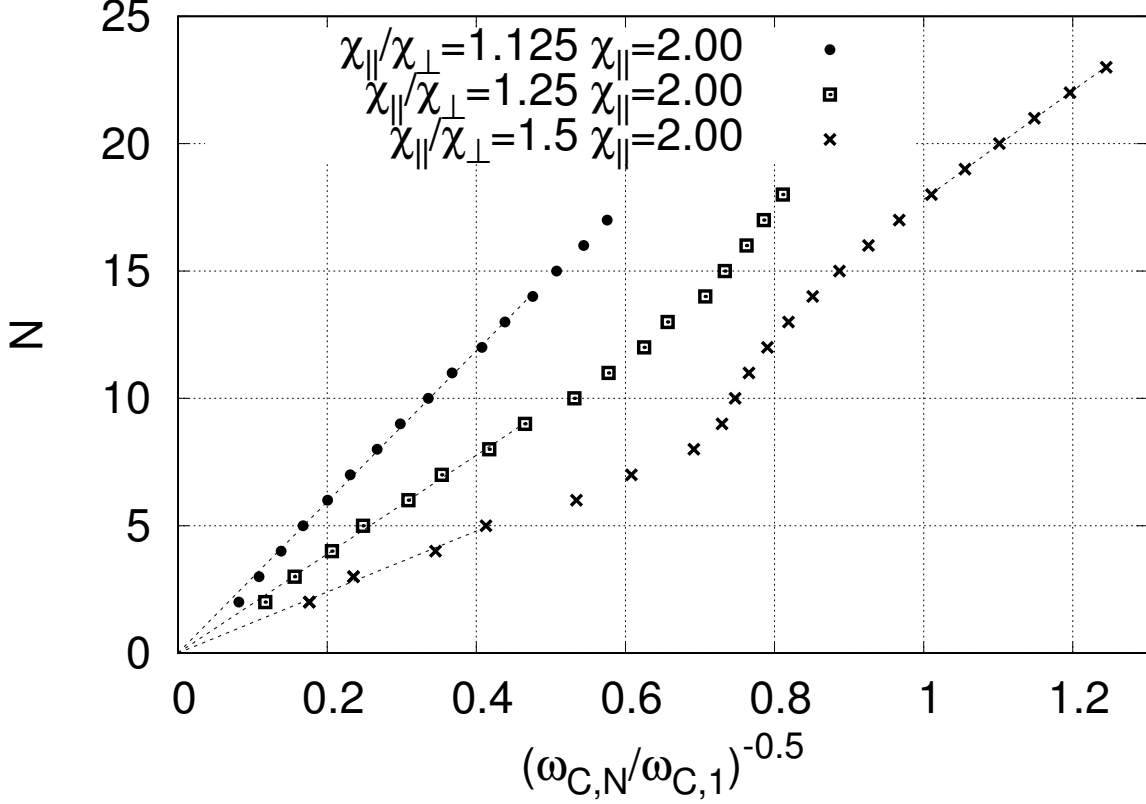


FIG. 7. The chain length  $N$  as a function of  $\sqrt{\frac{\omega_{C,1}}{\omega_{C,N}}}$  for chains with different magnetic anisotropy properties. Linear fit to  $N \propto \frac{1}{\sqrt{\omega_{C,N}}}$  in mode 4. and mode 1. shown as dotted lines.

Similarly critical chain length is proportional to  $\frac{1}{\sqrt{\omega_{C,N}}}$  in mode 1., where particles have large magnetic anisotropy and  $\frac{\omega_{C,N}}{\omega_{C,1}} < 1$ . Linear fit in mode 1. is shown in Fig. 8. These findings agrees with theory from section III.

In modes 2. and 3. critical chain length deviates from proportionality to  $\frac{1}{\sqrt{\omega_{C,N}}}$  as can be seen in Fig. 7 and Fig. 8 for  $\frac{\omega_{C,N}}{\omega_{C,1}}$  values close to unity.

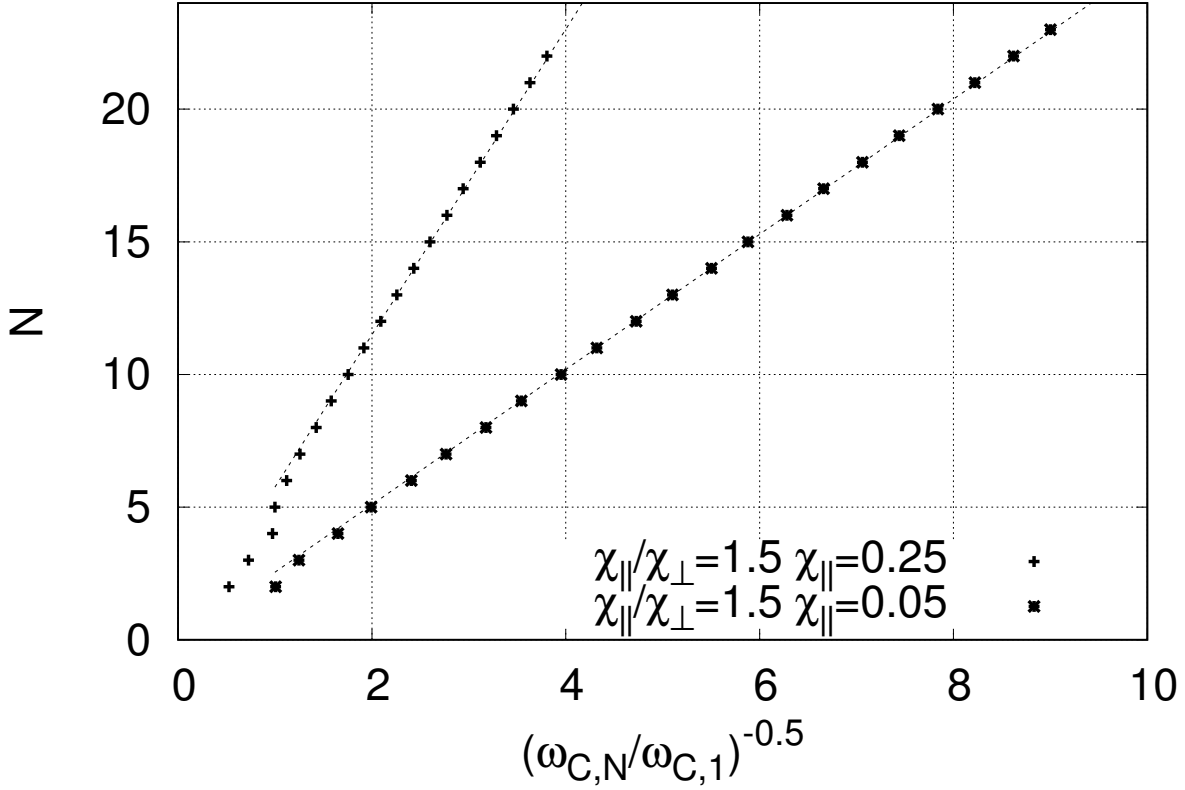


FIG. 8. The chain length  $N$  as a function of  $\sqrt{\frac{\omega_{C,1}}{\omega_{C,N}}}$  for chains with different magnetic anisotropy properties. Linear fit to  $N \propto \frac{1}{\sqrt{\omega_{C,N}}}$  in mode 1. shown as dotted lines.

### C. Distribution of chain lengths in an ensemble

If at the beginning the particles are randomly distributed and a rotating field is being applied then particles get organized in planes, where distribution of chain lengths can be observed. If  $r_{max}$  is smaller than  $\sqrt{5}R$  particles create chains with width larger than 1 and other other large structures. The region where  $r_{max} > \sqrt{5}R$  is not studied. If  $r_{max}$  value is larger than  $\sqrt{5}R$ , in simulations  $r_{max} = 2.3R$ , particles create one particle thick chains. Chains rotate next to each other, collide and exchange with particles. As a result, chains of different length can be observed. Length of each chain is being measured and a chain length distribution is obtained. If the distance between two particles is less than  $2.1R$  then they are being considered neighbors. If a particle has one neighbor then it is an end particle of a chain. If a particle has two neighbors then it is one of the middle particles of the chain. If a particle has more than two neighbors then the structure is not a 1 particle thin chain



and all the neighboring particles are excluded from the chain distribution results. This gives algorithm to obtain chain length distribution.

The development of distribution of chains lengths can be seen in Fig. 9 for particle parameters  $\frac{\chi_{\parallel}}{\chi_{\perp}} = 1.5$  and  $\chi_{\parallel} = 0.25$  at field frequency  $\frac{\omega_H}{\omega_{C,1}} = 0.1$ . Histogram of chain lengths is obtained by counting chains over 400 subsequent periods and 100 frames in each period. As can be seen in histogram, in first 2000 periods typical chain length of 12 particles developed.

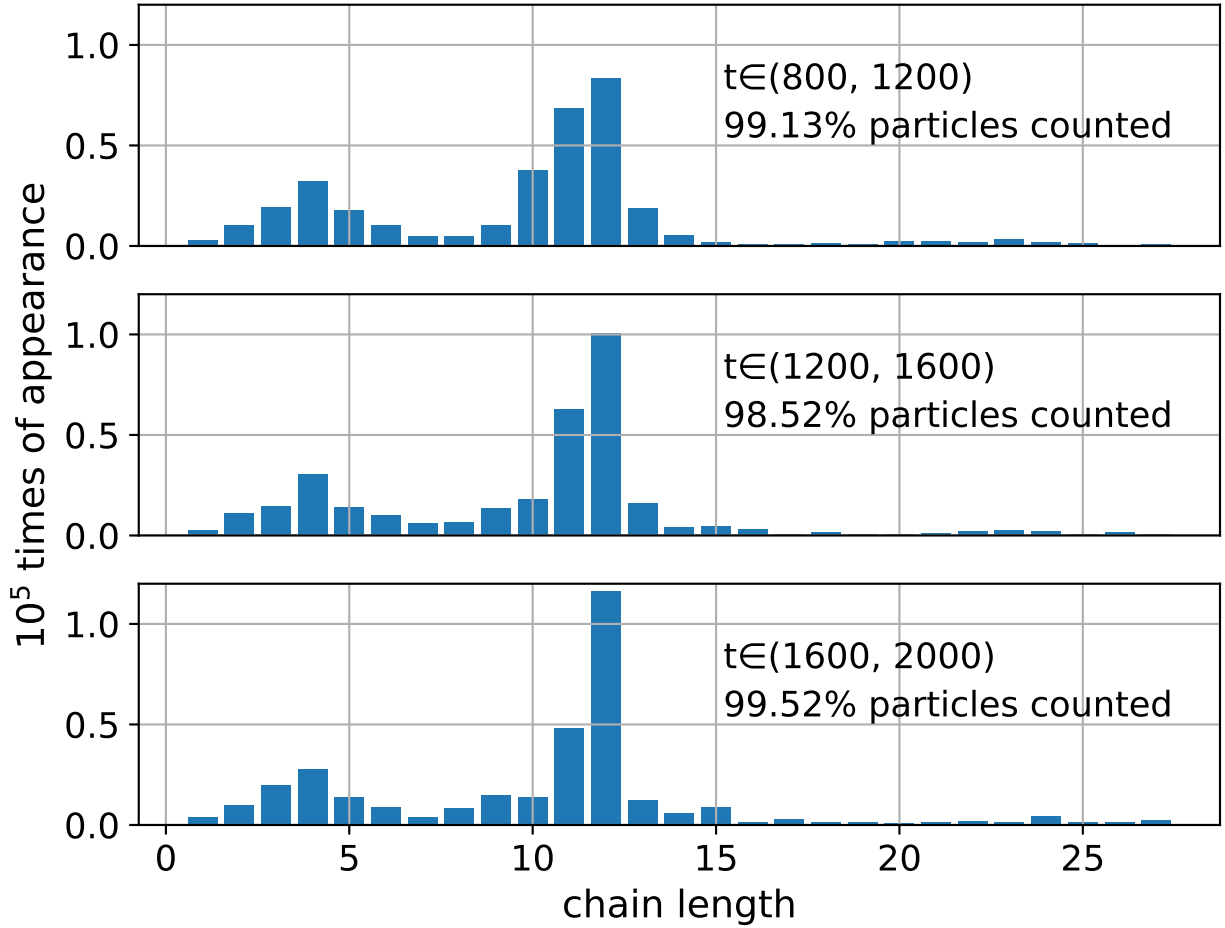


FIG. 9. Chain length distribution development over time in an ensemble of chains. Simulation gives typical ensemble chain length  $N_{ensemble} = 12 \pm 0.5$ . Initially 91 particle were randomly distributed in a plane. Each histogram contains the sum of chain length distribution histograms for 400 field rotation periods and 100 frames per period.  $\frac{\chi_{\parallel}}{\chi_{\perp}} = 1.5$  and  $\chi_{\parallel} = 0.25$  at field frequency  $\frac{\omega_H}{\omega_{C,1}} = 0.1$ .

In ideal case, infinite number of particle should be used in simulations, but simulations show that a couple of times more particles than the most popular chain length is enough

to get the distribution of chain lengths in ensemble. If more particles are being used or the initial layout of particles, or particles density are changed then only the time for reaching the stable configuration changes, but the final distribution of chains lengths is not changed.

In mode 1. there is a certain chain length that dominates in the distribution of chains lengths, but in all other modes the width of the dominating peak is larger. The error is being calculated as a half width at half maximum.

The ratio between critical chain length of single chain and typical chain length in ensemble of chains has been calculated. Numerical simulations show that critical and typical ensemble chain length ratio is constant for certain type of particle as can be seen in Fig. 10 graphs A1, A2, B1 and B2. Ratio mean values coincide within its standard deviations in cases A1 and B1 ( $1.65 \pm 0.06$  for A1 and  $1.68 \pm 0.07$  for B1). For larger  $\chi_{||}$  the ratio between critical and typical chain length decrease, as can be seen in Fig. 10 graph A2 (mean value  $1.57 \pm 0.07$ ) and B2 (mean value  $1.48 \pm 0.15$ ). Graph B2 includes particle motion not only in mode 1., but also modes 2.b and 3. In this case the ratio does not change much as the modes change. For larger frequencies error bars are longer because the chains are shorter and in asynchronous regime the ensemble chain distribution is wider.

In figures A3 and B3 Fig. 10 typical chain length in an ensemble becomes close to critical chain length and the ratio becomes one. The ratio becomes one if critical chain length is in mode 2.a. The mode 2.a can be observed in A3 and B3 Fig. 10 for frequencies up to  $\frac{\omega_H}{\omega_{C,1}} = 1.79$  in graph A3 and up to  $\frac{\omega_H}{\omega_{C,1}} = 1.72$  in graph B3. If the frequency is increased, the mode 2.a gradually changes to mode 3., and the ratio becomes larger. The explanation for the fact that in mode 2.a typical chain length becomes equal to typical chain length in ensemble could be following: In ensemble, when two identical chains meet with each other, for a moment they form one twice as long chain, in mode 2.a the chain will split in half because only the end particles of these two chains were disorientated. Unlike in all other modes where all the particle have similar disordered state and have more equal probability become the breaking point.

Rotation frequencies in Fig.10 were chosen to coincide with critical frequencies which for most of the parameters can be found in Fig.6.

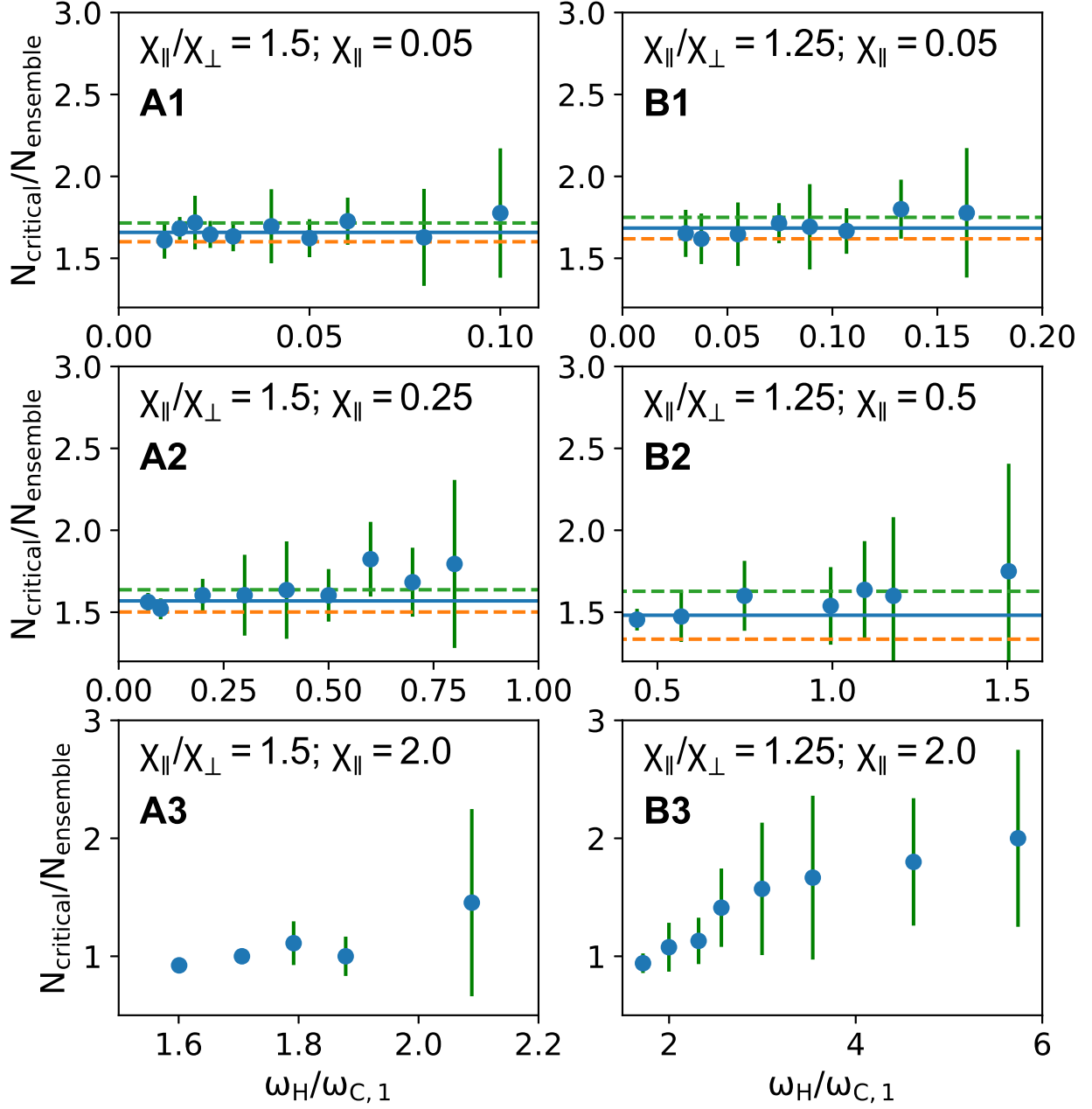


FIG. 10. Ratio of one chain critical length and chain ensemble typical length  $\frac{N_{\text{critical}}}{N_{\text{ensemble}}}$  for particles with different magnetic properties. Weighted mean value of ratio is illustrated as a solid line and weighted standard deviation is illustrated with dashed line. Ratios in graphs A1, A2, B1 and B2 are constant within standard deviations. Ratios in graphs A1 and B1 coincide within standard deviation. The larger magnetic susceptibility the smaller the ratio is.

## V. CONCLUSIONS AND DISCUSSION

Numerical simulations show that critical chain length dependence on field frequency for paramagnetic particles with magnetic anisotropy obeys trend observed for isotropic particles if the field frequency is not close to critical frequency of individual particle  $\omega_{C,1}$ . For both particles, magnetically isotropic and anisotropic, critical chain length in rotating field can be approximated as a function inverse proportional to square root of rotation frequency  $N \propto \frac{1}{\sqrt{\omega_H}}$ . The deviation from this trend for paramagnetic particles with magnetic anisotropy is the highest if rotation frequency is slightly above critical frequency of individual particle  $\omega_{C,1}$ . There is a small difference in the proportionality factor in  $N \propto \frac{1}{\sqrt{\omega_H}}$  above and below critical frequency  $\omega_{C,1}$ . In conclusion, the observation of critical chain length does not allow to identify that the particles have magnetic anisotropy if the field frequency is not close to the critical frequency of individual particle  $\omega_{C,1}$ .

In ensemble of chains typical chain length is smaller than the critical chain length of the single chain, for the same frequency. Simulations show that typical chain length is 1.5 times smaller than the critical chain length. The exception is situation where only two end particles of the single chain rotate asynchronously with the field, when the field frequency is close to critical. In this situation, typical chain length is almost equal to critical chain length. This can be observed if the rotation frequency is slightly higher than the critical frequency of an individual particle  $\omega_{C,1}$  and particles have high magnetic susceptibility. As a result, the fact that the chain length in ensemble is smaller than the critical chain length should be considered, when comparing a theory with an experiment.

In low frequency regime, where field rotation frequency  $\omega_H$  is smaller than the critical frequency of an individual particle  $\omega_{C,1}$ , and particles rotate synchronously with the field, distribution of chain lengths in ensemble is narrower than in high frequency range, where  $\omega_H > \omega_{C,1}$ . All particles, which has anisotropy, will rotate slowly and the chain length distribution will expand. Therefore, to create large amount of paramagnetic chains with equal length it is better to use paramagnetic particles with magnetic anisotropy than magnetically almost isotropic particles.

## VI. ACKNOWLEDGMENTS

This work was supported by PostDoc Latvia  
[Project no. 1.1.1.2/VIAA/1/16/060].

- 
- [1] B. Yigit, Y. Alapan, and M. Sitti, Cohesive self-organization of mobile microrobotic swarms, *Soft Matter* **16**, 1996 (2020).
  - [2] H. Massana-Cid, F. Meng, D. Matsunaga, R. Golestanian, and P. Tierno, Tunable self-healing of magnetically propelling colloidal carpets, *Nature Communications* **10**, 2444 (2019).
  - [3] K. Han, G. Kokot, S. Das, R. G. Winkler, G. Gompper, and A. Snezhko, Reconfigurable structure and tunable transport in synchronized active spinner materials, *Science Advances* **6**, 10.1126/sciadv.aaz8535 (2020), <https://advances.sciencemag.org/content/6/12/eaaz8535.full.pdf>.
  - [4] S. Melle and J. E. Martin, Chain model of a magnetorheological suspension in a rotating field, *The Journal of Chemical Physics* **118**, 9875 (2003), <https://doi.org/10.1063/1.1570817>.
  - [5] Y. Gao, M. A. Hulsen, T. G. Kang, and J. M. J. den Toonder, Numerical and experimental study of a rotating magnetic particle chain in a viscous fluid, *Phys. Rev. E* **86**, 041503 (2012).
  - [6] A. Vázquez-Quesada, T. Franke, and M. Ellero, Theory and simulation of the dynamics, deformation, and breakup of a chain of superparamagnetic beads under a rotating magnetic field, *Physics of Fluids* **29**, 032006 (2017), <https://doi.org/10.1063/1.4978630>.
  - [7] M. DEVI, P. P. DUTTA, and D. MOHANTA, Analytical calculation of chain length in ferrofluids, *Bulletin of Materials Science* **38**, 221 (2015).
  - [8] W. Lo, C. Lu, C. Lin, and C. Chen, Trajectory of a non-magnetic particle transported by a rotating magnetic particle chain, *IEEE Transactions on Magnetics* **55**, 1 (2019).
  - [9] A. Cēbers and I. Javaitis, Dynamics of a flexible magnetic chain in a rotating magnetic field, *Phys. Rev. E* **69**, 021404 (2004).
  - [10] S. L. Biswal and A. P. Gast, Rotational dynamics of semiflexible paramagnetic particle chains, *Physical review. E, Statistical, nonlinear, and soft matter physics* **69**, 041406 (2004).
  - [11] P. Tierno, Recent advances in anisotropic magnetic colloids: realization, assembly and applications, *Phys. Chem. Chem. Phys.* **16**, 23515 (2014).

- [12] A. Stikuts, R. Perzynski, and A. Cēbers, Spontaneous order in ensembles of rotating magnetic droplets, *Journal of Magnetism and Magnetic Materials* **500**, 166304 (2020).
- [13] C.-Y. Chen, H.-C. Hsueh, S.-Y. Wang, and Y.-H. Li, Self-assembly and novel planetary motion of ferrofluid drops in a rotational magnetic field, *Microfluidics and Nanofluidics* **18**, 795 (2015).
- [14] F. Martinez-Pedrero, A. Ortiz-Ambriz, I. Pagonabarraga, and P. Tierno, Colloidal microworms propelling via a cooperative hydrodynamic conveyor belt, *Phys. Rev. Lett.* **115**, 138301 (2015).
- [15] A. Aharoni, *Introduction to the Theory of Ferromagnetism*, International Series of Monographs on Physics (Clarendon Press, 2000).
- [16] A. Mukhtar, K. Wu, X. Cao, and liyuan Gu, Magnetic nanowires in biomedical applications, *Nanotechnology* **31**, 433001 (2020).
- [17] E. Yammine, E. Souaid, S. Youssef, M. Abboud, S. Mornet, M. Nakhil, and E. Duguet, Particles with magnetic patches: Synthesis, morphology control, and assembly, *Particle & Particle Systems Characterization* **37**, 2000111 (2020), <https://onlinelibrary.wiley.com/doi/pdf/10.1002/ppsc.202000111>.
- [18] E. C. S. S. F.R.S., Xcvii. the demagnetizing factors for ellipsoids, *The London, Edinburgh, and Dublin Philosophical Magazine and Journal of Science* **36**, 803 (1945), <https://doi.org/10.1080/14786444508521510>.
- [19] J. Čimurs, A. Brasovs, and K. Ērglis, Stability analysis of a paramagnetic spheroid in a precessing field, *Journal of Magnetism and Magnetic Materials* **491**, 165630 (2019).
- [20] B. Frka-Petesic, K. Erglis, J. Berret, A. Cēbers, V. Dupuis, J. Fresnais, O. Sandre, and R. Perzynski, Dynamics of paramagnetic nanostructured rods under rotating field, *Journal of Magnetism and Magnetic Materials* **323**, 1309 (2011), proceedings of 12th International Conference on Magnetic Fluid.
- [21] M. Galassi *et al.*, Gnu scientific library reference manual (2018), <https://www.gnu.org/software/gsl/>.
- [22] Z. He and H. D. Robinson, Assembly and disorder dissipation in superparamagnetic nanoparticle chains in a rotating magnetic field (2020), arXiv:2003.03008.